ELSEVIER

Journal of Photochemistry and Photobiology A: Chemistry 120 (1999) 171–179

Journal of Photochemistry and Photobiology A:Chemistry

Excited state behaviour of pentahelicene dinitriles

Helmut Görner[a,*], Christian Stammel[b], Jochen Mattay[b,1]

[a]*Max-Planck-Institut für Strahlenchemie, Post Box 101365, D-45413, Mülheim an der Ruhr, Germany*
[b]*Insitut für Organische Chemie, Universität Kiel, Olshausenstr. 40, D-24098, Kiel, Germany*

Received 7 September 1998; received in revised form 16 October 1998; accepted 16 October 1998

Abstract

The excited singlet and triplet states 2,13-dicyano[5]helicene (**1**) and two *para*-dicyno[5]helicenes containing one and two methyl groups (**2** and **3**, respectively) were studied in solvents of different polarity as a function of temperature. Fluorescence quenching by electron donors such as triethyl amine indicated photoinduced electron transfer. In the absence of additives triplet states were observed by flash photolysis. The triplet lifetime at room temperature was rather short (<1 μs) and the decay limited by intramolecular processes, e.g. charge transfer in the cases of **2** or **3**. Luminescence of singlet molecular oxygen, $O_2(^1\Delta_g)$, was observed with moderate and low quantum yield for **1** and **3**, respectively. For **1–3**, the triplet lifetime increases by six orders of magnitude on going to −196°C. Two subsequently formed triplet states were observed for **3** at lower temperatures. The effects of temperature and solvent polarity on the quantum yields of fluorescence and phosphorescence and the spectroscopic and kinetic triplet absorption properties were examined. The influence of substituents on the deactivation pathways of excited pentahelicenes are discussed.

Keywords: Photophysics; Fluorescence quenching; Photoinduced electron transfer; Triplet state; Singlet oxygen; Quantum yields

1. Introduction

The first helicene was already synthesized 1956 by Newman and Lednicer [1] in 12 steps involving the racemic resolution of phenanthreno[3,4-c]phenanthrene. Although Martin and coworkers [2] developed the nowadays standard synthetic procedure in 1967, i.e. photochemical phenanthrene cyclization, and a huge variety of helicenes were synthesized in the following years [3–5], there are only few reports on substituted pentahelicenes. Katz et al. [6] reported 1997 on a new approach to synthesize pentahelicenes and hexahelicenes following the Diels–Alder methodology. The spectroscopic and photochemical properties of helicenes have been investigated over the years by several groups [7–11].

In the course of our studies directed towards the development of chiral photosensitizers in energy and electron transfer processes, we have recently synthesized various acceptor-substituted pentahelicenes [12,13]. Although photoinduced electron transfer represents a rapidly growing field in photochemistry [14–18], there are only a few reports on chiral sensitizers in asymmetric photoreactions [19,20]. Helicenes are of major interest since they can be separated into stable enantiomers and, as a consequence, might act as chiral phototsensitizers [20]. Rau and Totter [11] have recently studied the fluorescence quenching of enantiometric pure hexahelicene by *N*-methyl-*N*-(2-methylbutyl)-aniline leading to exciplex and ion pair formation. However, the authors observed only chiral discrimination of smaller than 1.3. No photophysical and photochemical studies on substituted pentahelicenes could be found in the literature.

In this paper, we report on the singlet and triplet state properties of three pentahelicenes substituted with cyano groups: 2,13-dicyano[5]helicene (**1**), 1,4-dicyano-13-methyl[5]helicene (**2**) and 11,14-dicyano-1,3-dimethyl[5]-helicene (**3**). The photophysical behaviour, e.g. fluorescence, phosphorescence, T–T absorption, was studied in solvents of different polarity, as well as some photochemical reactions (fluorescence quenching by amines). The effects of temperature and substituents on the deactivation pathways are discussed in detail.

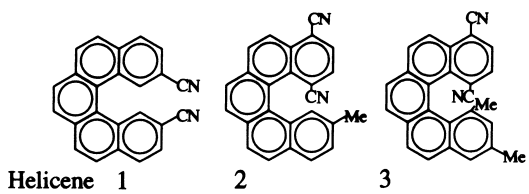

Helicene 1 2 3

*Corresponding author. Tel.: +49-208-306-3593; fax: +49-208-306-3951; e-mail: goerner@mpi-muelheim.mpg.de

[1]New address: Fakultät für Chemie, Universität Bielefeld, Postfach 100131, D-33501 Bielefeld, Germany

1010-6030/99/$ – see front matter
PII: S1010-6030(98)00423-7

2. Experimental details

The dicyano-substituted pentahelicenes were synthesized, on the basis of the well-known photochemical reaction of stilbene to phenanthrene [21], as described elsewhere [12,13]; the other compounds (Aldrich, Fluka) were used as supplied, e.g. 1,4-diazabicyclo[2.2.2]octane (DABCO), triethyl amine (TEA), tributyl amine (TBA), 1,2,4-trimethoxybenzene (TMB) and 1,1′-biphenyl (BP) or purified by distillation: *N*,*N*-dimethylaniline (DMA). The molar absorption coefficients of **1**, **2** and **3** in acetonitrile are $\varepsilon_{290} = 3.9 \times 10^4$, $\varepsilon_{285} = 3.2 \times 10^4$ and $\varepsilon_{295} = 4.0 \times 10^4$ $M^{-1}\,cm^{-1}$ [13]. The solvents (Merck) were purified by distillation: methylcyclohexene (MCH) and 2-methyltetrahydrofuran (MTHF) or used without further purification: toluene, acetonitrile (Uvasol) and ethanol.

For measurements of the quantum yields Φ_f and Φ_p, optically matched solutions ($A = 0.4$ per cm at 330 nm, 1.0 and 0.4 cm path length at 24 and −196°C, respectively) and 9,10-diphenylanthracene as reference ($\Phi_f = 1.0$ at −196°C) were used and the corrected emission spectra were recorded on a Spex-Fluorolog. Since quenching by oxygen reduces both Φ_f and τ_f, the fluorescence intensities were measured in argon, air and oxygen-saturated solutions and the fluorescence lifetimes (τ_f) and, as an example, the Φ_f values in acetonitrile at room temperature were corrected accordingly. The experimental error in Φ_f and Φ_p is ±25%, those in τ_f, τ_p and τ_T are typically ±20, ±15 and ±10%, respectively.

Three excimer lasers (Lambda Physik) and the third harmonic of a neodymium laser (J.K. Lasers) (pulse width 10–20 ns) were used for excitation at 193, 248, 308 and 354 nm, respectively. The laser photolysis setup was essentially the same as described elsewhere [22–25]. The absorbance of the samples at the excitation wavelength was 0.5–2 (in the 1 cm cuvette) and only a minor part of the excitation light was absorbed within a 0.5 mm layer near the front wall of the cell which, in turn, was probed by the monitoring beam orthogonal to the excitation beam. Typical pentahelicene concentrations for $\lambda_{exc} = 248$, 308 and 354 nm were 0.03, 0.05 and 0.1–0.2 mM, respectively. Data registration and analyses were performed by two transient digitizers (Tektronix 7912AD and 390AD) and a computer (Acorn 540). The temperature of the sample was monitored by a thermocouple. The output at 248 or 308 nm was also used for measurements of the phosphorescence lifetimes.

Luminescence of singlet molecular oxygen at 1269 nm [26–32] was detected after the pulse using a cooled Ge detector (North Coast, EO 817FP), a silicon and an interference filter and two amplifiers (Comlinear, CLC-103). The signal, which is overlapped by fluorescence extending even to 1269 nm (and some additional scatter), was extrapolated to the end of the 20 ns pulse (I_Δ). At a fixed laser intensity I_Δ was found to show a linear dependence on either the absorbed energy, being proportional to $(1–10^{-A})$, or on I_L with a curvature at higher intensities; the slope of the latter plot is denoted as q_Δ. The quantum yield of formation of $O_2(^1\Delta)_q$ in benzene was obtained from q_Δ values using optically matched solutions ($A_{308} = 0.6$) and 2-acetonaphthone as reference $\Phi_\Delta^{ref} = 0.84$ [30]. For the values in other oxygen-saturated solvents a correction has to be applied using the rate constant for radiative deactivation of $O_2(^1\Delta_g)$ (k_r) relative to that in benzene (k_r^0).

$$\Phi_\Delta = \Phi_\Delta^{ref} \times \left(\frac{q_\Delta}{q_\Delta^{ref}}\right)\left(\frac{k_r^0}{k_r}\right) \quad (1)$$

3. Results and discussion

3.1. Fluorescence and phosphorescence properties

The emission spectra of the pentahelicenes in glassy media at −196°C show two main bands which are attributed to fluorescence and phosphorescence. Examples are shown in Fig. 1(a)–(c) for **1**, **2** and **3**, respectively. For **1** in MCH as non-polar solvent both bands are structured with maxima (λ_f and λ_p, respectively) at 442 and 566 nm; similar spectra were monitored in solvents of medium and large polarity. The spectra of **2** and **3** are comparable, albeit the latter shows only little structure (Table 1). Owing to the electron accepting cyano and electron donating methyl groups of **3**, one could expect intramolecular charge transfer (CT) interaction. Indeed, for **3** λ_f is red-shifted from 463 nm in MCH to 520–530 nm in acetonitrile or ethanol, whereas virtually no shift appears for **1** on changing the polarity. At room temperature only fluorescence remains.

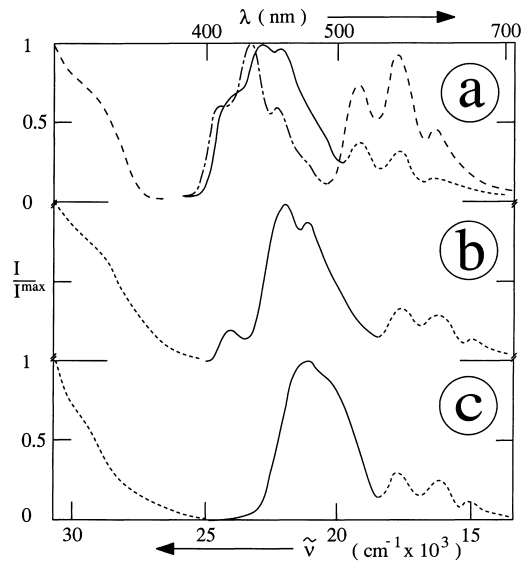

Fig. 1. Phosphorescence excitation spectrum (left, $\lambda_{obs} = 570$ nm) and fluorescence and phosphorescence spectra (middle and right, respectively, $\lambda_{exc} = 330$ nm) of (a) **1** in MCH (full and dotted line) and EtOH (broken lines), (b) **2** in MTHF and (c) **3** in EtOH at −196°C.

Table 1
Maxima and quantum yields of fluorescence and phosphorescence[a]

Compound	Solvent	Temperature (°C)	λ_f [b] (nm)	λ_p (nm)	Φ_f	Φ_p
1	MCH	24	415, 429, 463		0.02	
		−196	420, 442, 459	524, 566, 610	0.11	0.01
	Toluene	24	416, 435, 458		0.04	
	MTHF	−196	415, 435, 460	532, 572, 620	0.12	0.03
	Acetonitrile	24	415, 430, 456		0.03 (0.054)[c]	
	Ethanol	24	413, 430, 458		0.03	
		−196	412, 430, 456	527, 570, 620	0.12	0.10
2	MCH	24	[430], 450, 478			
		−196	[421], 477	560	0.10	<0.01
	MTHF	24	[425], 485			
		−196	[435], 458, 485			
3	MCH	24	463, 482			
		−196	482, 500	563, 615		
	Toluene	24	488		0.04	
	MTHF	−196	470, 500	564, 615	0.12	0.02
	Acetonitrile	24	520		0.03 (0.038)	
	Ethanol	24	530		0.03	
		−196	470, 500	564, 616	0.12	0.02

[a]In air-saturated solution, $\lambda_{exc} = 330$ nm.
[b]Maximum values are underlined. Values in brackets denote weak shoulder.
[c]Values corrected for deoxygenated conditions are indicated in parentheses.

The excitation spectra at −196°C of fluorescence (not shown) and phosphorescence (Fig. 1) steadily decrease on going from 300 to 400 nm. This is in agreement with the absorption spectra which were measured at room temperature. The energies of the S_1 state of **1** and **3** are about 292 and 270 kJ mol^{-1}, respectively. Note that the absorption of helicenes extends toward 450–470 nm [8]. The quantum yields of fluorescence (Φ_f) and phosphorescence (Φ_p) under the various conditions are compiled in Table 1. The highest Φ_p value was found for **1** in ethanol.

The two emission bands of the three pentahelicenes are also distinguished by strongly differing lifetimes (τ_f and τ_p, respectively). The decay kinetics of the excited singlet state can be fitted by a monoexponential major component (and a minor second one). The lifetime at 24°C for **1** in air-saturated MCH, acetonitrile and ethanol, is $\tau_f = 9.0$, 6.2 and 8.4 ns, respectively (Table 2), and those for **2** and **3** are similar or slightly smaller. The τ_f values are 5–8 ns (main component) for **1**–**3** in ethanol at −196°C. The phosphorescence lifetime (or at least the longest living component) approaches values around 1 s at −196°C, e.g. for **1**, **2** and **3** in MTHF, $\tau_p \approx 1.0$, 0.9 and 1.0 s, respectively, or in ethanol $\tau_p \approx 1.2$, 0.8 and 0.8 s, respectively.

3.2. Fluorescence quenching

From fluorescence quenching of **1** and **3** by TEA in solvents of different polarity at room temperature, linear Stern–Volmer plots were obtained. Using the Stern–Volmer constant (K_{SV}) and the fluorescence lifetime, the rate constant for quenching (k_q) was found to be close to the diffusion-controlled limit for **1** and **3** in acetonitrile and smaller in solvents of lower polarity (Table 2). For **2** in toluene and acetonitrile, however, the Stern–Volmer dependence of fluorescence quenching by TEA are not linear (upward curved) and we did not undertake any investigations to elucidate the role of static quenching. K_{SV} values were also obtained for **1** and **3** in acetonitrile from linear Stern–Volmer plots as a function of the DABCO and DMA concentrations. For **1** and TEA in solvents of low polarity, weak exciplex fluorescence with maximum at 540 nm in MCH and at 560 nm in toluene was reported [13]. Exciplex fluorescence around 530 nm has also been found for a hexahelicene amine system in solvents of medium polarity, where the k_q values increase with increasing the solvent polarity approaching 5×10^9 M^{-1} s^{-1} for DABCO or DMA in acetonitrile [11].

1,1′-biphenyl (BP) has been shown in various systems to enhance the yield of oxidation products in the presence of a suitable electron donor [24,25,33,34]. The catalytic role of BP can be described by electron transfer from BP to the excited singlet state of the acceptor, thereby forming $BP^{\bullet+}$ and the radical anion ($A^{\bullet-}$), and the subsequent electron transfer from the applied donor to $BP^{\bullet+}$. Unfortunately, for **1** and **3** in acetonitrile, formation of $BP^{\bullet+}$ was not achieved due to the too small k_q value of $<2 \times 10^7$ M^{-1} s^{-1}, i.e. fluorescence quenching by BP is unsuccessful. From this one would postulate that the redox properties of **1** and **3** are similar. However, the measured reduction potential of the two acceptors is quite different, $E_{red} = -1.7$ and −1.3 V

Table 2
Rate constant for fluorescence quenching[a]

Helicene	Solvent	τ_f [b] (ns)	Donor [c]	K_{SV} (M^{-1})	K_q ($M^{-1}\,s^{-1} \times 10^9$)
1	MCH	12 (9.0)	TEA	6.7	0.6
	Toluene		TEA	8.6	
	Acetonitrile	8.2 (6.2)	DABCO	50	6
			DMA	60	7.3
			TEA	47	5.7
			TBA	30	3.7
			TMB	40	5
			biphenyl	<0.2	<0.02
	Ethanol	12 (8.4)	TEA	7.6	0.6
2	Acetonitrile	7.1 (5.7)	TEA	d	
	Ethanol		TEA	6	
3	MCH	5.0 (4.3)	TEA	18	4
	Toluene		TEA	14	
	Acetonitrile	6.4 (5.4)	DABCO	65	10
			DMA	70	11
			TEA	31	5
			TBA	13	2
			TMB	32	5
			biphenyl	<0.2	<0.03
	Ethanol	4.9 (4.2)	TEA	5.7	1.2

[a]In air-saturated solution at 24°C. Lifetimes are corrected for oxygen free solution. $\lambda_{exc} = 360$–380 nm.
[b]Experimental values in air-saturated solution are given in parentheses.
[c]E_{ox} (in V): DABCO (0.57), *N*,*N*-dimethylaniline (DMA, 0.7), triethyl amine (TEA, 0.8), tributyl amine (TBA, 0.82), 1,2,4-trimethoxybenzene (TMB, 1.1), biphenyl (1.8).
[d]No linear dependence.

(versus Ag/AgCl [13]) or −2.14 and −1.72 V (versus ferrocene [35]) for **1** and **3**, respectively. Using the values for the S_1 state it follows that the reduction potential (versus SCE) in the excited singlet state is $E^*_{red} \approx 1.0$ and ≈1.1 V for **1** and **3**, respectively. For comparison, $E^*_{red} = 1.4$ and 1.9 V for 9-cyanoanthracene and 9,10-dicyanoanthracene, respectively [25]. The oxidation potential of the donors used ranges from $E_{ox} \approx 0.7$ V for DMA to 1.8 V for BP. The k_q values of the amines (Table 2) are in agreement with the Rehm–Weller relationship [36,37].

$$\Delta G = E_{ox} - E^*_{red} - E_c \quad (2)$$

Here, ΔG is the free energy change for electron transfer and the term E_c accounting for ion pairing (0.06 V in acetonitrile). For example, with **1** $\Delta G = -0.3$ V for DMA and 0.8 V for BP.

3.3. Triplet state properties

For each of the three pentahelicenes examined, a transient absorption was observed at the end of the laser pulse. The absorption spectrum of **1** in argon-saturated MTHF at room temperature shows two transients with maxima (λ_{TT}) at 420 and 680 nm (Fig. 2(a)). They are produced during the excitation pulse (or appear after the fluorescence peak) and the decay follows first-order kinetics with lifetimes(τ_T)1 of 110 ns in the blue and of about 70 ns in the red spectral region. Essentially the same absorption spectra with two main bands centered at 410–430 and 680–700 nm and similar decay kinetics as in MTHF were observed in solvents of low and high polarity (Table 3).

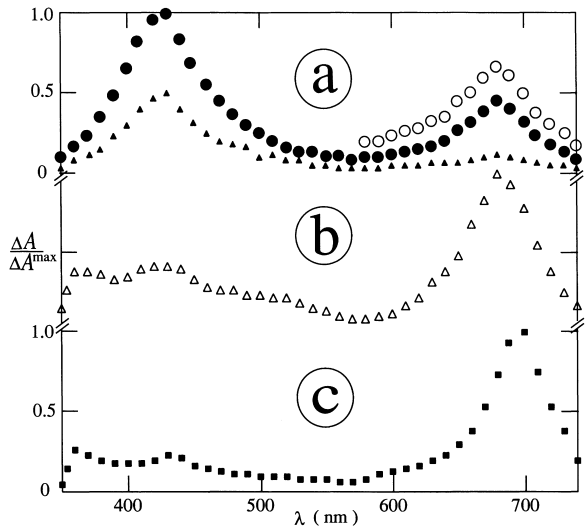

Fig. 2. T–T absorption spectra of **1** in argon-saturated MTHF at (a) 24°C, 30 ns (○), 60 ns (●) and 150 ns (▲) after the 308 nm pulse; (b) −50°C and (c) −170°C ca. 1 μs after the 308 nm pulse.

Table 3
T–T absorption maxima and triplet lifetime[a]

Helicene	Solvent	Temperature (°C)	λ_{TT} [b] (nm)	τ_T (μs)
1	MCH	24	410, 670	0.12/0.05[c]
	MTHF	24	420, 680	0.11/0.07[c]
		−100	420, 700	200
		−170	430, 700	(>0.3)[d]
	Acetonitrile[e]	24	410, 690	0.08/0.05[c]
	Ethanol	24	420, 690	0.09/0.05[c]
		−100	420, 700	200
		−170	420, 700	(>0.3)
2	MCH	24	400, 560	0.18
	MTHF	24	410, 600	0.18
		−170	510, 710	(>0.2)
	Acetonitrile[e]	24	410, 650	0.2
	Ethanol	24	410, 660	0.20
		−100	500	0.7
		−170	500	(>0.6)
3	MCH	24	430, 600	0.95
		−100	385, 670[f]	
	MTHF	24	400, 600	0.90
		−100	380, 670[f]	
		−170	520	(>0.2)
	Acetonitrile[e]	24	410, 600	1.0
	Ethanol	24	410, 600	0.95
		−100	390, 670[f]	
		−170	520, 700	(>0.2)

[a]In argon-saturated solution; $\lambda_{exc} = 308$ nm unless otherwise indicated.
[b]Maximum underlined.
[c]Two lifetimes refer to respective maxima.
[d]Lifetimes in parentheses refer to s (not μs).
[e]Same results with $\lambda_{exc} = 248$ or 354 nm.
[f]Two subsequent components, see text.

Both transients are assigned to triplet states on the basis of the following findings: (1) The transients are quenched by oxygen, the rate constant in acetonitrile is $k_{ox} = 3 \times 10^9\ M^{-1}\ s^{-1}$, based on the lifetimes at 430 nm in the absence and presence of air. (2) The $1/\tau_T$ value strongly decreases with increasing $1/T$ and at −196°C it approaches the 0.5–1 s range, i.e. the time domain where τ_T is close or equal to τ_p (Fig. 3). (3) In MTHF (Fig. 2(a)) or ethanol at −170°C the triplet–triplet (T–T) absorption spectrum extends from 360 nm with maximum at $\lambda_{TT} = 700$ nm and the same lifetime in the whole spectrum. Interestingly, the T–T absorption spectrum of parent pentahelicene also extends over the whole visible spectral range [10]. A common triplet lifetime at 420 and 680 nm can be observed for **1** even at higher temperatures, e.g. $\tau_T = 0.2$ ms in ethanol at −100°C (Table 3). In MTHF or ethanol the ΔA_{680} value increases and approaches about sixfold higher value on going from 25 to −100°C, whereas the ΔA_{420} value remains relatively constant over the whole temperature range. This indicates two pathways for triplet population (see Section 3.5).

The properties of the triplet state(s) of the two other pentahelicenes are similar to those of **1** in as much as (1) the decay follows first-order kinetics, (2) the lifetime is

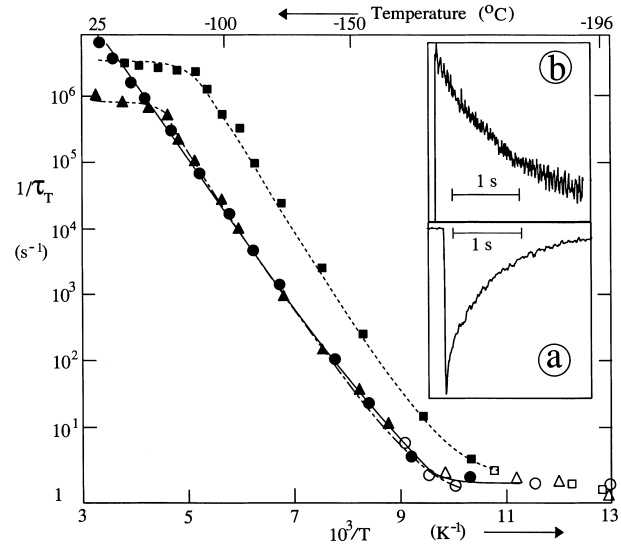

Fig. 3. Temperature dependence of log of the reciprocal triplet lifetime for **1** (circles, full line), **2** (squares, dotted line) and **3** (triangles, dashed line) in argon-saturated MTHF. Full symbols: rate constant for decay of the T–T absorption at 400 nm, $\lambda_{exc} = 308$ nm. Open symbols: reciprocal phosphorescence lifetime. Insets: signals of **1** at −175°C; (a) phosphorescence and (b) absorption.

rather short at room temperature, (3) the transient in solution at room temperature is efficiently quenched by oxygen and (4) $1/\tau_T$ decreases by 6–7 orders of magnitude with decreasing temperature between 24 and −196°C (Fig. 3). On the other hand, the triplet properties of **2** and **3** are different in several aspects. Only one triplet state was observed in acetonitrile at room temperature. The rate constant for quenching by oxygen is $k_{ox} = (6–9) \times 10^9\ M^{-1}\ s^{-1}$, i.e. larger than for **1** and close to the diffusion-controlled limit. For **2** the T–T absorption spectrum contains only one major band centred at 410 nm at room temperature (Fig. 4(a)). At lower temperatures the spectrum covers the whole visible spectrum with $\lambda_{TT} = 500$ nm (Fig. 4(b) and (c)).

The T–T absorption spectrum of **3** is even more sensitive to variation of temperature and/or viscosity. It shows a maximum at 400 nm at ambient temperatures under all conditions used, e.g. in MTHF with $\lambda_{exc} = 354$ nm (Fig. 5(a)) or in ethanol with $\lambda_{exc} = 248$ nm (Fig. 6(a)). The absorption spectrum broadens when the glasses become rigid with $\lambda_{TT} = 520$ nm (Fig. 5(c) and Fig. 6(c)). Closer inspection of the decay kinetics of **3** in MCH, MTHF or ethanol at temperatures between −90 and −140°C (Table 3) reveals that the triplet with the 400 nm band is the precursor of a second triplet with maxima at 380 nm and around 670 nm. The conversion of the first into the second triplet is illustrated in the insets of Fig. 7(a). These results indicate the existence of a total of three triplet configurations of **3**, one (T_{410}) at higher temperatures (Fig. 5(a)), one in the glassy media (Fig. 5(c) and Fig. 6(c)) and another ($T_{380/670}$), formed subsequently from the initial triplet, in a certain intermediate temperature range (Fig. 5(b), Fig. 6(a) and (b) and Fig. 7(a)). The rate constant of the grow-in kinetics of **3**

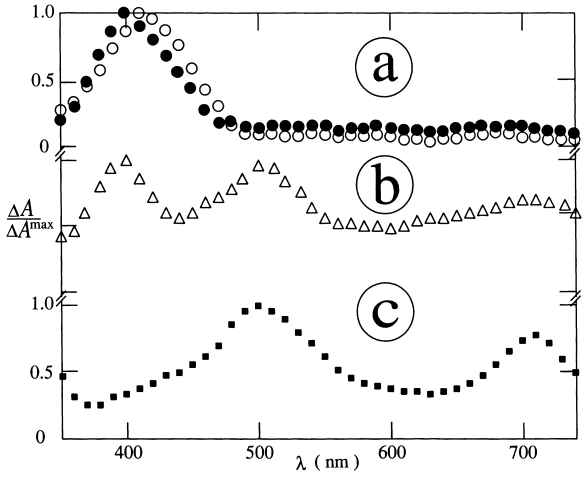

Fig. 4. T–T absorption spectra of **2** in argon-saturated MTHF at (a) 25°C and −10°C (full and open symbols, respectively) 0.1 μs after the 308 nm pulse; (b) −90°C and (c) −170°C ca. 1 μs after the 308 nm pulse.

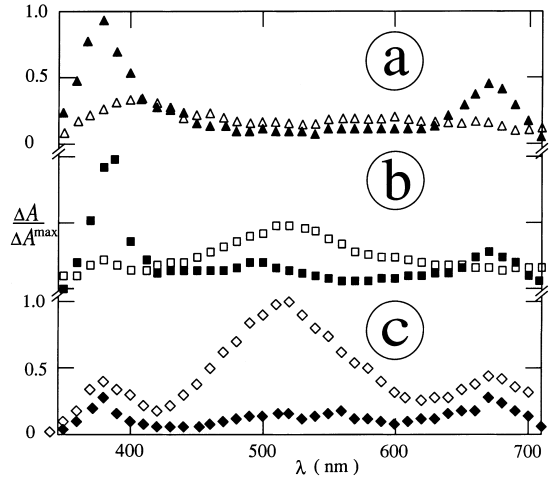

Fig. 6. T–T absorption spectra of **3** in argon-saturated ethanol at (a) −70°C, 0.1 and 1 μs (b) −140°C, <1 μs and 100 μs and (c) −160°C <1 ms and 50 ms after the 248 nm pulse (open and full symbols, respectively).

increases with increasing $1/T$ and is roughly one order of magnitude larger than that of the decay (Fig. 7(b)).

Compared to the significant temperature-dependent changes in ΔA_{680} of **1** those of **2** and **3** are smaller. A further difference is a steady decrease in the semi-logarithmic plot of $1/\tau_T$ with increasing $1/T$ for **1** and a rather small change at higher temperatures for **2** and partly for **3** (Fig. 3). The short triplet lifetime of the three dicyano-substituted pentahelicenes at room temperature with respect to that of phenanthrene or other helicenes [9] indicates an intramolecular deactivation process for triplet decay.

Several quenching measurements were carried out with **3**, where τ_T is largest at room temperature. Almost no quenching effect by DABCO, TEA and DMA was found in argon-saturated acetonitrile. With these three additives electron transfer in the triplet state is unlikely; for the rate constant an upper limit of $k_q = 2 \times 10^6\ M^{-1}\ s^{-1}$ was estimated. Energy transfer from the triplet state of **3** to 1,3-cyclohexadiene in toluene or acetonitrile is also inefficient, the rate constant was estimated to be smaller than $1 \times 10^6\ M^{-1}\ s^{-1}$. This is consistent with triplet energies of about 213 and 219 kJ mol^{-1} for **3** and 1,3-cyclohexadiene, respectively. for comparison, energy transfer from the triplet state of 9-cyanophenanthrene (triplet energy of 250 kJ mol^{-1}) to 1,3-cyclohexadiene takes place; in toluene $k_q > 4 \times 10^8\ M^{-1}\ s^{-1}$. Preliminary results with **1**, concerning the dimerization of 1,3-cyclohexadiene in acetonitrile show an *exo* : *anti* : *syn* ratio of 1 : 3 : 1, indicating an energy transfer from **1** to the diene [13].

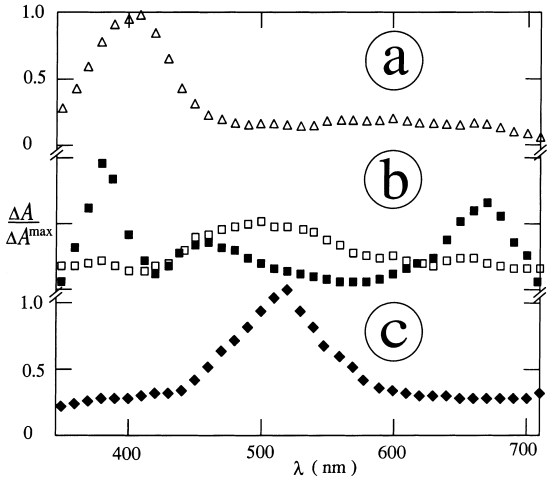

Fig. 5. T–T absorption spectra of **3** in argon-saturated MTHF at (a) 25°C, and 0.1 μs; (b) −110°C and at <1 μs and 100 μs (open and full symbols, respectively); (c) −170°C and 1 μs after the 354 nm pulse.

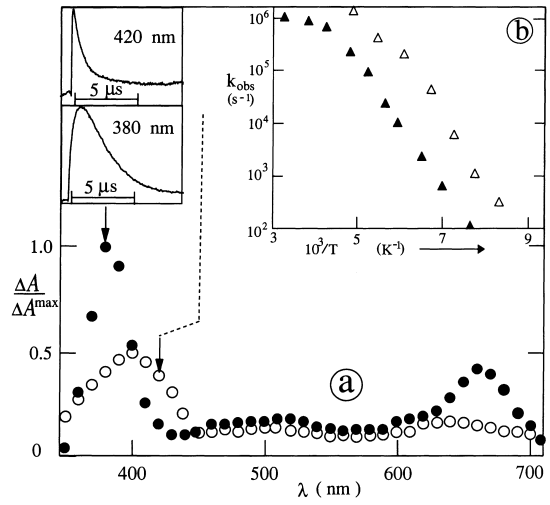

Fig. 7. Spectrum and kinetics of **3** in argon-saturated MTHF (a) T–T absorption spectra at −80°C at the end of the 308 nm pulse (open circles) and after 1 μs (full circles). Insets: kinetics at 380 and 420 nm; (b) rate constants for decay at 420 nm and grow-in at 380 nm (full and open triangles, respectively) as a function of $1/T$.

It should be noted that neither the radical anion of a pentahelicene nor a radical cation of an amine could be observed using conditions of 50–90% fluorescence quenching and $\lambda_{exc} = 354$ nm. The radical cation of DMA could be observed independently via photoionization (either in the absence or presence of a pentahelicene) using $\lambda_{exc} =$ 248 nm or 308 nm. The reason for the lack of observation of the radical anion of a pentahelicene is probably the low value of its absorption coefficient and the much larger value of T–T absorption. For **3** and KI in ethanol–water mixtures (1 : 9) the radical anion was generated by reaction with the solvated electron which, in turn, was generated by photoionization of I^- using $\lambda_{exc} = 193$ nm. The spectrum of $\mathbf{3}^{\bullet -}$ has maxima at 320 and 440 nm and the estimated absorption coefficient is $\leq 5 \times 10^3\ M^{-1}cm^{-1}$. For comparison, the absorption coefficient of the radical anion of 9,10-dicyanoanthracene at 312 and ≈500 nm is 9×10^4 and $\leq 4 \times 10^3\ M^{-1}\ s^{-1}$, respectively [24,25].

3.4. Singlet molecular oxygen

Formation of $O_2(^1\Delta_g)$ was detected upon excitation of **1** and **3** in several air or oxygen-saturated solvents. Examples of its decay are shown in Fig. 8 for **1** and **3** in toluene. The luminescence lifetime (τ_Δ) is characteristic for each solvent, e.g. 30 μs in benzene, shorter in alcohols and longer in most other solvents (Table 4). Generally, no significant dependence of τ_Δ on I_L was found except in CCl_4 where the lifetime was limited by trace impurities (and a second shorter-lived decay component appeared at $I_L > 3$ MW cm^{-2}). Therefore, the intensity was kept below this level. Because of the rather short triplet lifetime in the absence of oxygen, the signal increases strongly when the air-saturated sample is purged by oxygen; this is expressed by the Φ_Δ(air)/$\Phi_\Delta(O_2)$ ratio.

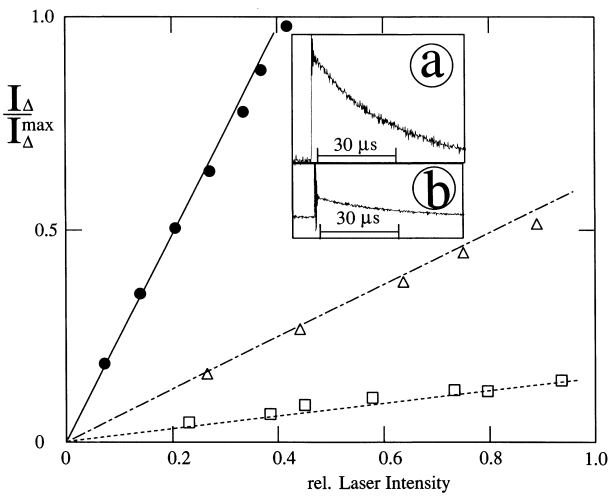

Fig. 8. Luminescence intensity of $O_2(^1\Delta g)$ extrapolated to the 308 nm pulse end as a function of the laser intensity for **1** (triangles, inset a) and **3** (squares, inset b) in toluene and 2-acetonaphthone in benzene (●).

Table 4
Lifetime, relative rate constant, ratio in air vs. oxygen-saturated solution and quantum yield if $O_2(^1\Delta_g)$ formation[a]

Solvent	τ_Δ (μs)	$k_r/k_r^{o\,b}$	Φ_Δ(air)/ $\Phi_\Delta(O_2)$ **1**	Φ_Δ(air)/ $\Phi_\Delta(O_2)$ **3**	Φ_Δ **1**	Φ_Δ **3**
Cyclohexane	25	0.44	0.34	0.4	0.35	0.07
CCl_4	500	0.62			0.3	
Toluene	28	0.96	0.26	0.3	0.22	0.05
Benzene	30	1.0	0.24	0.3	0.16	0.04
Dioxane	25	0.37			0.13	
Dichloromethane	100	0.24	0.33	0.5	0.22	0.02
Acetonitrile	65	0.30				<0.03

[a]Using $\lambda_{exc} = 308$ nm.
[b]Taken from [30–32], see text.

For the two pentahelicenes in several solvents and for 2-acetonaphthone in benzene as reference, the signals, extrapolated to the pulse end (I_Δ), depend for a given concentration linearly on the incident laser intensity (Fig. 8). The quantum yield of $O_2(^1\Delta_g)$ formation (Φ_Δ) was obtained from the slopes for optically matched samples using Eq. (1). The k_r/k_r^0 ratios were taken from the literature [30–32]. In each case the Φ_Δ values (Table 4) are the lower limit for the quantum yield of intersystem crossing (Φ_{isc}).

3.5. Deactivation pathways

Helicenes show generally a small or moderate quantum yield of fluorescence ($\Phi_f = 0.01$–0.1) and a high Φ_{isc} value (0.8–0.9) [8]. The phosphorescence spectra of the three dicyano-substituted pentahelicenes (Fig. 1) are reminiscent to that of parent pentahelicene, where in non-polar glasses a lifetime of 2–3 s, $\Phi_p = 0.15$ and a significantly higher Φ_{isc} value (above 0.8) has been reported [10]. For the dicyano compounds fluorescence is also a minor pathway (Table 1). A Φ_{isc} value of 0.5–0.8 is conceivable, but radiationless deactivation bypassing the triplet state cannot be excluded. The onset of the fluorescence and phosphorescence spectra are separated by an energy gap of ca. 5000 cm^{-1}, corresponding to about 296 and 238 kJ mol^{-1}, respectively, for the S_1 and T_1 states of **1**. The energy levels of the S_1 and T_1 states of **3** are about 270 and 215 kJ mol^{-1}, respectively, and those of **2** are in between these values.

It should be recalled that for each of the three pentahelicenes the solvent polarity has no significant effect on the spectral and kinetic features of the triplet state(s) and their temperature dependence. Also a change of the excitation wavelength from 248 to 308 mm and even to 354 nm has no obvious effect on the features of the triplet state(s). For hexahelicenes it has been shown that variation of λ_{exc} between 260 and 390 nm has no influence on the phosphorescence to fluorescence ratio [11]. The triplet lifetime of **1**–**3** at room temperature is short and independent of solvent polarity (Table 3), indicating triplet decay via intramolecular deactivation processes. From the linear plot of log $1/\tau_T$

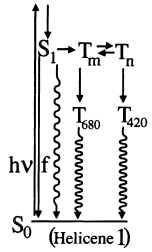

Scheme 1.

versus $1/T$ in MTHF (Fig. 3) an activation energy of 25 kJ mol^{-1} and an A-factor of 5×10^{10} s^{-1} are obtained.

The nature of the triplet configurations remains open as yet, but their appearance in media of low, medium and high polarity points to an intramolecular origin rather than to a solvent rearrangement. The strong increase of ΔA_{680} for **1** in MTHF or ethanol on cooling (see 3.3.) indicates two pathways for triplet population (Scheme 1): One strongly temperature-dependent step towards T_{680} which originates from the S_1 state after intersystem crossing into an upper excited triplet state (denoted as T_m) and the second step towards T_{420} originating from another precursor, probably from an higher excited triplet equilibrium, e.g. $T_m \rightleftarrows T_n$. A shift of such a triplet equilibrium from the T_n side at higher temperatures towards the T_m side may account for the observed spectral changes (Fig. 2). This hypothesis differs from the model for pentahelicene, where the primary triplet state is that from the parent compound itself and the subsequent one has tentatively been assigned to that of the dihyrobenzoperylene [10]. Also for **1** cyclization is, in principle, possible, but no sequence of triplet states could be observed.

A specific rearrangement in the triplet moiety becomes detectable for **3** at lower temperatures, but still in rather fluid media (Figs. 4–7). One conceivable interpretation for the two subsequently formed triplet states of **3** in MCH, MTHF or ethanol at lower temperatures is the existence of an equilibrium between T_{410} and $T_{380/670}$ (Scheme 2). At higher temperatures the observed species is T_{410}, while the decay of $T_{380/670}$ is faster than its formation. At lower temperatures the proposed triplet equilibrium is no longer established, e.g. because the $T_{380/670} \rightarrow T_{410}$ step is slower than the competing intersystem crossing step. For **3** CT, due to the electron accepting and donating groups, and steric hindrance of the methyl and cyano groups should be largest. The hypothesis

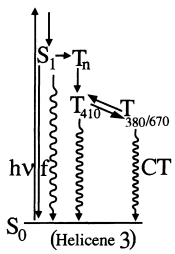

Scheme 2.

for CT in the cases of **2** and **3** is difficult to verify since the triplet lifetime of **3** over a wide temperature range is similar to **1** (Fig. 3) and largest at higher temperatures.

In summary, we report on new deactivation pathways without precedence in the literature for three dicyano-substituted pentahelicenes which, however, should be further examined. For **1**, where cyclization is possible, an equilibrium between two upper excited triplet states could account for the formation of two observable triplet states at ambient temperatures. On the other hand, for **3**, where cyclization is not possible, two triplet states in equilibrium at ambient temperatures and their subsequent formation at low temperatures is proposed. Concerning the role of these compounds for initiation of a charge or electron transfer reaction in the excited singlet state, it seems that the application is limited to electron donors with an oxidation potential of smaller than ca. 1.4 V. Likewise, the rather low triplet energies limit their use for energy transfer.

Acknowledgements

We thank Professor K. Schaffner for his generous support, Mrs. G. Klihm, E. Hüttel and Mr. L.J. Currell for technical assistance and the State of North-Rhine Westfalia and the Fonds der Chemischen Industrie for financial support.

References

[1] M.S. Newman, D.J. Lednicer, J. Am. Chem. Soc. 78 (1956) 4765.
[2] N. Flammang-Barbieux, J. Nasielsky, R.H. Martin, Tetrahedron Lett. 8 (1967) 746.
[3] W.H. Larhoven, W.J.C. Prinsen, Top. Curr. Chem. 125 (1984) 63.
[4] F.B. Mallory, C.W. Mallory, Org. Reactions 30 (1984) 1.
[5] W.H. Laarhoven, Org. Photochem. 10 (1989) 163.
[6] T.J. Katz, L. Liu, N.D. Willmore, J.M. Fox, A.L. Rheingold, S. Shi, C. Nuckolls, B.H. Rickman, J. Am. Chem. Soc. 119 (1997) 10054.
[7] J.B. Birks, D.J.S. Birch, E. Cordemans, E. Vander Donckt, Chem. Phys. Lett. 43 (1976) 33.
[8] M. Sapir, E. Vander Donckt, Chem. Phys. Lett. 36 (1975) 108.
[9] I. Carmichael, G.L. Hug, J. Phys. Chem. Ref. Data 15 (1986) 1.
[10] K.-H. Grellmann, P. Hentschel, T. Wismintski-Knittel, E. Fischer, J. Photochem. 11 (1979) 197.
[11] H. Rau, F. Totter, J. Photochem. Photobiol. A: Chem. 63 (1992) 337.
[12] C. Stammel, R. Fröhlich, J. Mattay, H. Wenck, A. de Meijere, Eur. J. Org. Chem., submitted.
[13] C. Stammel, Ph.D. Thesis, University of Münster, 1995.
[14] M. Schmittel, A. Burghart, Angew. Chem. Int. Ed. Engl. 36 (1997) 2550.
[15] G. Pandey, Top. Curr. Chem. 168 (1993) 175.
[16] J. Mattay, Angew. Chem. Int. Ed. Engl. 26 (1987) 825.
[17] S. Hintz, A. Heidbreder, J. Mattay, Top. Curr. Chem. 177 (1996) 77.
[18] F. Müller, J. Mattay, Chem. Rev. 93 (1993) 99.
[19] Y. Inoue, Chem. Rev. 92 (1992) 741.
[20] J. Mattay, M. Vondenhof, Top. Curr. Chem. 159 (1991) 219.
[21] P. Hugelshofer, J. Kalvoda, K. Schaffner, Helv. Chim. Acta 43 (1960) 1322.

[22] J. Gersdorf, J. Mattay, H. Görner, J. Am. Chem. Soc. 109 (1987) 1203.
[23] K.-D. Warzecha, M. Demuth, H. Görner, J. Chem. Soc., Faraday Trans. 93 (1997) 1523.
[24] H. Görner, K.-D. Warzecha, M. Demuth, J. Phys. Chem. 101 (1997) 9964.
[25] K.-D. Warzecha, H. Görner, M. Demuth, J. Chem. Soc., Faraday Trans. 94 (1998) 1701.
[26] F. Wilkinson, W.P. Helman, A.B. Ross, J. Phys. Chem. Ref. Data 22 (1993) 113.
[27] R.W. Redmond, S.E. Braslavsky, Chem. Phys. Lett. 148 (1988) 523.
[28] F. Wilkinson, W.P. Helman, A.B. Ross, J. Phys. Chem. Ref. Data 24 (1995) 663.
[29] G. Martinez, S.G. Bertolotti, O.E. Zimerman, D.O. Martire, S.E. Braslavsky, N.A. Garcia, J. Photochem. Photobiol. B: Biol. 17 (1993) 247.
[30] R.D. Scurlock, S. Nonell, S.E. Braslavsky, P.R. Ogilby, J. Phys. Chem. 99 (1995) 3521.
[31] R.D. Scurlock, P.R. Ogilby, J. Phys. Chem. 91 (1987) 4599.
[32] R. Schmidt, E. Afshari, J. Phys. Chem. 94 (1990) 4377.
[33] J. Eriksen, C.S. Foote, J. Phys. Chem. 82 (1978) 2659.
[34] I.R. Gould, D. Ege, E.J. Moser, S. Farid, J. Am. Chem. Soc. 112 (1990) 4290.
[35] E. Bothe, private communication.
[36] D. Rehm, A. Weller, Isr. J. Chem. 8 (1970) 259.
[37] D. Rehm, A. Weller, Ber. Bunsenges. Phys. Chem. 73 (1969) 834.